

## Controlling Stochastic Resonance

Luca Gammaitoni,<sup>1</sup> Markus Löcher,<sup>4</sup> Adi Bulsara,<sup>2</sup> Peter Hänggi,<sup>3</sup> Joseph Neff,<sup>4</sup>

Kurt Wiesenfeld,<sup>4</sup> William Ditto,<sup>4</sup> and Mario E. Inchiosa<sup>2</sup>

<sup>1</sup>*Dipartimento di Fisica, Università di Perugia and Istituto Nazionale di Fisica Nucleare, Sezione di Perugia, I-06100 Perugia, Italy*

<sup>2</sup>*Space and Naval Warfare Systems Center San Diego, Code D-364, San Diego, California 92152-5001*

<sup>3</sup>*Institut für Physik, Universität Augsburg, Lehrstuhl für Theoretische Physik I, D-86135 Augsburg, Germany*

<sup>4</sup>*School of Physics, Georgia Institute of Technology, Atlanta, Georgia 30332-0430*

(Received 22 January 1999)

We introduce an open-loop control scheme for stochastic resonators; the scheme permits the enhancement or suppression of the spectral response to threshold-crossing events triggered by a time-periodic signal in background noise. The control is demonstrated in experiments using a Schmitt trigger. A generic two-state theory captures the essential features observed in our experiments and in numerical simulations; this suggests the generality of the effect. [S0031-9007(99)09258-3]

PACS numbers: 05.40.Ca, 02.50.Ey, 47.20.Ky, 85.25.Dq

Stochastic resonance (SR) is a nonlinear noise-mediated cooperative phenomenon wherein the coherent response to a deterministic signal can be enhanced in the presence of an optimal amount of noise. Since its inception in 1981 [1], SR [2] has been demonstrated in diverse systems including sensory neurons, mammalian neuronal tissue, lasers, SQUIDS, tunnel diodes, and communications devices. Variations and extensions of the classical definition of SR to include aperiodic (e.g., dc or wideband) signals, with the detector response quantified by various information-theoretic [3] or spectral cross-correlation [4] measures, have also appeared in the literature.

In this Letter, we introduce a control scheme which allows us, at will, to either enhance or suppress the spectral response in the basic SR effect. Our control strategy is applicable when input information is transmitted via the crossing of either a threshold or potential energy barrier. This raises the intriguing possibility that in situations where external signals might be potentially deleterious, e.g., electromagnetic field interactions with neuronal tissue [5], their effects could be substantially reduced or even eliminated via (externally applied) control signals.

The experiments were carried out in a modified Schmitt trigger (ST) electronic circuit. The Schmitt trigger is one of the simplest threshold systems [6,7], possessing a static hysteretic nonlinearity. We denote the lower and upper threshold voltages in the Schmitt trigger by  $V_L$  and  $V_U$ , respectively, with  $2b$  being the (static) threshold separation. A subthreshold 64 Hz time-sinusoidal signal  $S(t) = A_S \sin \omega_S t$  ( $A_S < b$ ) and Gaussian noise [8] are applied to the input. For fixed, equal and opposite  $V_L$  and  $V_U$ , standard SR curves can be obtained by measuring the output signal power (SP) at the fundamental frequency  $\omega_S$  as a function of input noise power [9]. To realize the control scheme we modulate the upper and lower thresholds sinusoidally,  $V_U(t) = b + A_M \sin(\omega_M t + \phi)$ ,  $V_L(t) = -V_U(t)$ , which results in a

“breathing” oscillation (Figs. 1 and 2) of the barriers with frequency  $\omega_M$ . We keep the signal and threshold modulating amplitudes fixed such that  $A_M + A_S < b$  (no deterministic switching) and investigate the system’s response as a function of the phase offset  $\phi$  and the input noise power. Note that in this work we only consider integer frequency ratios  $n = \omega_M / \omega_S (= 1, 2)$ .

Our experimental results are shown in the gray-scale plots of Fig. 3, where signal output power (SP) is gray-scale encoded as a function of the phase and input noise power. Analogous results are obtained if the output signal-to-noise ratio (SNR) is taken as the measure of the response. Figure 3(a) is simply the classic SR case [2] with no control ( $A_M = 0$ ): The signal output power

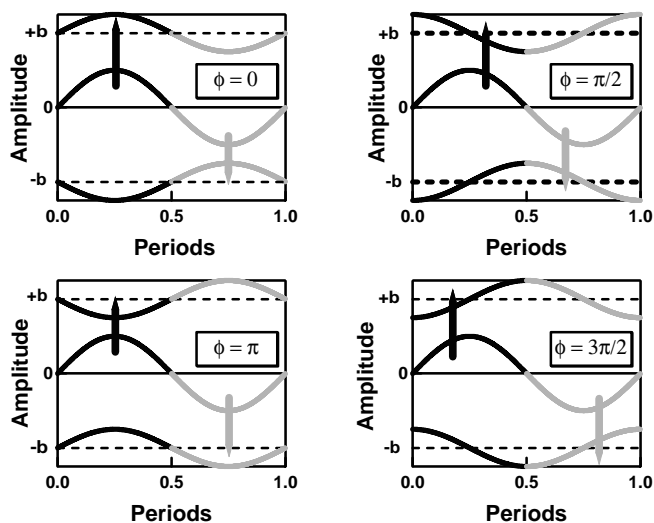


FIG. 1. The input signal  $S(t)$  (middle trace) relative to the modulated upper and lower thresholds for four different phases. The two frequencies are identical:  $\omega_M = \omega_S$ . Black and gray distinguish the first and second halves of the drive cycle. The arrows indicate the most likely times of switching events.

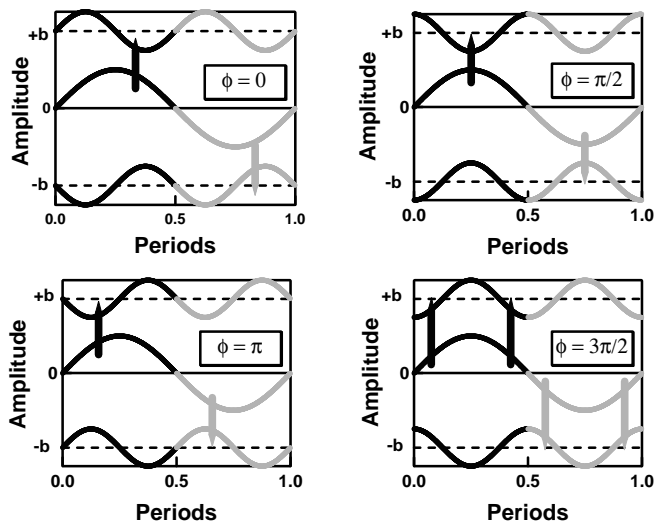


FIG. 2. Same as Fig. 1, but with  $\omega_M = 2\omega_S$ .

passes through a maximum at an optimal noise intensity, with the location of the maximum depending strongly on the internal parameters, as well as the input signal amplitude  $A_S$ , but relatively weakly on the signal frequency  $\omega_S$ , provided this frequency lies well within the device bandwidth. For this case, the output power spectral density (PSD) is known to consist of peaks at the odd multiples of the signal frequency, superimposed on a Lorentzian-like noise background. Dips (corresponding to power absorption) can also occur (last reference in [2]) in the PSD at high input SNRs. In the modulated-threshold case the output PSD displays a more complex sequence of interrelated peaks and dips, occurring at frequencies  $|m\omega_M \pm n\omega_S|$  ( $m, n$  integers), with properties that depend on the input SNR, the symmetry of the device, the noise statistics, and the threshold separation and modulation amplitude. Note that, if the signal is weak and the barrier modulation strong, dips appear in the PSD at the harmonics of the barrier frequency  $\omega_M$ .

Figures 3(b) and 3(c) pertain to two different modulated-threshold cases, with  $\omega_M = \omega_S$  and  $\omega_M = 2\omega_S$ , respectively. The most striking feature of Fig. 3(b) is a significant *suppression* of the output signal power below its value in the nonmodulated case [Fig. 3(a)], at values 0 and  $\pi$  of the control phase  $\phi$ . As we will show below, to lowest order in the modulation amplitudes, no enhancement of the signal output power is to be expected. Note also that the plot appears symmetric with respect to a phase translation of  $\pi$ . A suppression behavior is also present in the case where  $\omega_M = 2\omega_S$  for  $\phi = 3\pi/2$  [Fig. 3(c)]; however, in this case, a significant enhancement of the output SP (compared to the nonmodulated case) is also evident at phase  $\phi = \pi/2$ .

We can get a qualitative understanding of the observed effects by plotting  $V_U(t)$ ,  $V_L(t)$ , and  $S(t)$  on the same graph. Maximum enhancement (suppression) of the switching process will take place when the extrema of

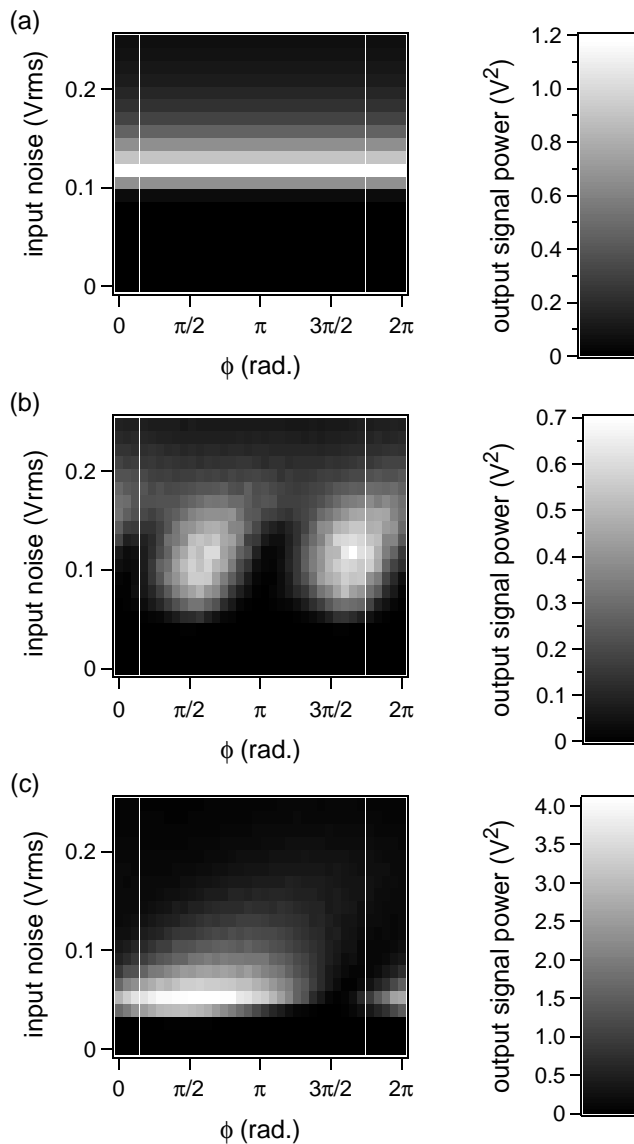


FIG. 3. Linear gray-scale plot of output signal power[9] at  $\omega_S$  vs phase and noise for (a) no modulation, (b)  $\omega_M = \omega_S$ , and (c)  $\omega_M = 2\omega_S$ . Parameters:  $\omega_S = 64$  Hz,  $b = 300$  mV,  $A_M = 200$  mV, and  $A_S = 30$  mV. The output voltage of the Schmitt trigger is  $\pm 9$  V. In (b), the maximum signal enhancement occurs near  $\phi = \pi/2$  and  $\phi = 3\pi/2$ , and the maximum suppression occurs near phases  $\phi = 0$  and  $\phi = \pi$ . In (c), the maximum signal enhancement occurs near  $\phi = \pi/2$ , and the maximum suppression occurs near  $\phi = 3\pi/2$ . Note the differing signal output power gray scales shown in (a)–(c).

the modulation signal are exactly out of (in) phase with the extrema of the input signal  $S(t)$ . The relevant parameter is the distance between the signal and the thresholds: The transition probability in the presence of noise depends (inversely) exponentially on this distance. Figures 1 and 2 depict the cases  $\omega_M = \omega_S$  and  $\omega_M = 2\omega_S$ , respectively. The positions of the arrows indicate the points of closest approach, i.e., the points in a cycle at which transitions (direction symbolized by the arrow orientation) are

most likely. (Note that  $A_S > A_M$  in Figs. 1 and 2, while  $A_S < A_M$  in Fig. 3. For  $A_S < A_M$ , the points of closest approach to the upper and lower thresholds would shift to the opposite halves of the drive cycles in the  $\phi = 0$  and  $\phi = \pi$  panels, respectively, of Fig. 1.)

In one full switching cycle, both an upper threshold crossing and a lower threshold crossing must occur. If the distance of closest approach to either the lower or upper threshold is large, the cycling rate will be severely depressed; thus, to facilitate cycling, the maximum distance of closest approach must be minimized. In Fig. 1, this minimization occurs for phases  $\phi = \pi/2$  and  $\phi = 3\pi/2$ , yielding an optimal coherence between the output and input of the device (albeit, with a phase shift). For these phases, the effective threshold is identical for both extrema of the drive cycle, while for  $\phi = 0$  and  $\phi = \pi$ , transitions at one extremum are favored at the cost of the other. In fact, denoting the signal separations from the upper and lower thresholds by the quantities  $f_1(t, \phi) \equiv V_U(t) - S(t)$  and  $f_2(t, \phi) \equiv S(t) - V_L(t)$ , one can separately plot the values of the minima of the distances  $f_{1,2}(t)$  vs the phase offset  $\phi$ , in the absence of noise and assuming suprathreshold signals. For the  $\omega_M = \omega_S$  scenario, the two curves intersect at  $\phi = \pi/2, 3\pi/2$  in the interval  $0 \leq \phi \leq 2\pi$ ; these points correspond precisely to the locations of the maxima in the output signal power, within this simple phenomenological picture.

While the  $\omega_M = \omega_S$  case does not yield (at least for the parameters of Fig. 3) an enhancement in the output SP over the nonmodulated case, the SP enhancement in the case of  $\omega_M = 2\omega_S$  (Fig. 2) is significant. This is because, for the unique phase difference  $\phi = \pi/2$ , the effective threshold is significantly reduced at both extrema of the input signal (the  $\pi$  symmetry is absent in this case). Note that the maximum value of the SP from Fig. 3(c) is a sizeable  $4.2V^2$  (6.15 dB) compared to  $0.7V^2$  (-1.24 dB) in Fig. 3(b). A geometric construction, similar to that outlined in the preceding paragraph, yields the values of the minima of the distances  $f_{1,2}(t, \phi)$

having only one intersection, at  $\phi = \pi/2$ , in the interval  $0 \leq \phi \leq 2\pi$ .

The choice of optimal phase is less apparent if the control goal is to suppress the SP rather than enhance the basic SR effect. For the  $\omega_M = \omega_S$  case, maximum suppression occurs for phases  $\phi = 0$  and  $\phi = \pi$ . Unlike the symmetric mechanism that leads to enhancement, Fig. 1 demonstrates that the effective threshold for the upward transition is different from the corresponding downward one. Since the transition rates vary inverse exponentially with barrier height, switching events corresponding to the larger effective threshold are significantly reduced leading to a net suppression of the signal output power. Figure 3(b) demonstrates that for phases  $\phi = 0$  and  $\phi = \pi$  the onset of detectable signal output power can be substantially shifted towards higher noise powers. For the  $\omega_M = 2\omega_S$  case, the symmetry of transitions within one cycle is recovered for all of the phases exhibited in Fig. 2. In particular, for  $\phi = 3\pi/2$  the closest approach to the threshold is seen to be significantly widened in the presence of the modulation signal. This explains the observed suppression in the experiment at that phase as shown in Fig. 3(c).

We now briefly outline the main results of a nonlinear response perturbation theory, which captures many of the observed experimental features. Denote the two states of the Schmitt trigger as  $\pm c$ , respectively. Following Ref. [7], we write the Schmitt trigger dynamics in two-state form in terms of evolution equations for the state probabilities  $p_{\pm}$  (the overdot denotes time differentiation):  $\dot{p}_+ = W_-(t)p_- - W_+(t)p_+ = -\dot{p}_-$ , where we assume that, in the adiabatic limit ( $\omega_{S,M}$  well below the trigger and noise bandwidths and the transition rates  $W_{\pm}$ ), the transition rates *out of* the  $\pm$  state are given by  $W_{\pm}(t) = f[\mu \pm \eta_S \sin \omega_S t + \eta_M \sin(\omega_M t + \phi)]$  [10]. The (dimensionless) parameters  $\mu$  and  $\eta_{S,M}$  correspond to the threshold  $b$  and signal/modulation amplitudes scaled by the input noise power. For small signal and threshold modulation  $\eta_{S,M} \ll 1$ , we can expand the rates  $W_{\pm}(t)$  in  $\eta_{S,M}$  and solve the two-state dynamics to find the output power at the signal frequency  $\omega_S$ :

$$P_1 = \frac{\pi c^2 \alpha_1^2 \eta_S^2}{\alpha_0^2 + \omega_S^2} \left[ 1 + \eta_M^2 \left\{ \frac{(\alpha_1^2 - \alpha_0 \alpha_2)(\alpha_0 \cos 2\phi - \omega_S \sin 2\phi)}{2\alpha_0(\alpha_0^2 + \omega_S^2)} - \left( \frac{\alpha_2}{\alpha_0} - \frac{3\alpha_3}{2\alpha_1} \right) \cos 2\phi - \frac{\alpha_2}{\alpha_0} + \frac{3\alpha_3}{\alpha_1} \right. \right. \\ \left. \left. - \frac{\alpha_0 \alpha_2}{\alpha_0^2 + \omega_S^2} + \frac{\alpha_1^2 - \alpha_0 \alpha_2}{\alpha_0^2 + 4\omega_S^2} \right\} + \frac{3\eta_S^2}{2} \left( \frac{\alpha_3}{\alpha_1} - \frac{\alpha_0 \alpha_2}{\alpha_0^2 + \omega_S^2} \right) \right] \quad (1)$$

for  $\omega_M = \omega_S$ , and

$$P_2 = \frac{\pi c^2 \alpha_1^2 \eta_S^2}{\alpha_0^2 + \omega_S^2} \left[ 1 - \eta_M \alpha_1 \left\{ \frac{\omega_S \cos \phi + \alpha_0 \sin \phi}{\alpha_0^2 + \omega_S^2} - \frac{2\alpha_2}{\alpha_1^2} \sin \phi \right\} \right] \quad (2)$$

for  $\omega_M = 2\omega_S$ . Here, the  $\alpha_n$  are the expansion coefficients  $\alpha_n = \frac{2(-1)^n}{n!} \frac{d^n f(\mu)}{d\mu^n}$ . For any specific system these coefficients are found via a formal expansion of the transition rates  $W_{\pm}$ . For the ST, these rates can be cast as

the inverses of the mean first passage times of a Brownian particle to an absorbing barrier at the switching threshold [7], provided the noise bandwidth is within that of the device.

The location of the extrema of  $P_{1,2}$  depends on the ratio  $\frac{\alpha_0}{\omega_S}$ , which itself is noise dependent. This explains the apparent “drift” of the maximum SP towards higher values for the phase with increasing noise in Figs. 3(b) and 3(c). Note that  $P_1$  is invariant with respect to phase shifts of  $\pi$  (equivalent to a sign change in  $\eta_M$ ), which is also apparent in Fig. 3(b). Conversely, changing the sign of  $\eta_M$  alters  $P_2$ .

Direct simulations of the rate equations have yielded convincing agreement with Eqs. (1) and (2).

In summary, we have demonstrated a general nonfeedback control scheme, which can both enhance the “classical” SR effect and also suppress the response to a weak signal, in experiments carried out on a generic stochastic resonator (a modified Schmitt trigger). Our experimental results are confirmed in computer simulations of the Schmitt trigger as well as in a potential double-well system. Our scheme relies on controlling the *phase* of the externally applied barrier modulation, which leads to a nonlinear frequency mixing effect. The control is expected to be realizable in a large class of nonlinear dynamic systems in which internal parameters are externally accessible. This stands in contrast to the case of multiple time-periodic signals applied additively at the input of a nonlinear device. In the latter case the output contains “combination resonances” of the input frequencies, with selection rules that depend on the symmetry of the device; these were discussed as early as the late 19th century by von Helmholtz [11]. With noise, one expects an SR effect at every combination tone; this has been demonstrated recently [12] in a very simple bistable system. The response to an input signal can be annulled trivially by adding an inverted copy of the signal at the input; however, the amplitudes must be identical. In contrast, the threshold or barrier modulation discussed in this Letter does not require amplitude matching. We believe that controlled SR may be useful in applications as diverse as the cancellation of power-line frequencies in very sensitive magnetic field sensing applications with superconducting quantum interference devices and vibration control in nonlinear mechanical devices, as well as in the context of electromagnetic field interactions with neuronal tissue [5], where control of internal thresholds is possible [13] and the selective suppression of specific frequencies could potentially be beneficial.

We acknowledge support from the Office of Naval Research, the Internal Research Program at SPAWAR

Systems Center San Diego, and a NICOP Grant (L. G.) from ONR-Europe.

- 
- [1] R. Benzi, A. Sutera, and A. Vulpiani, *J. Phys. A* **14**, L453 (1981); C. Nicolis and G. Nicolis, *Tellus* **33**, 225 (1981).
  - [2] For reviews, see K. Wiesenfeld and F. Moss, *Nature (London)* **373**, 33 (1995); A. Bulsara and L. Gammaitoni, *Phys. Today* **49**, No. 3, 39 (1996); L. Gammaitoni, P. Hänggi, P. Jung, and F. Marchesoni, *Rev. Mod. Phys.* **70**, 223 (1998). A complete bibliography can be found at <http://www.pg.infn.it/sr>
  - [3] M. Stemmler, *Network* **7**, 687 (1996); A. Bulsara and A. Zador, *Phys. Rev. E* **54**, 2185 (1996); C. Heneghan *et al.*, *Phys. Rev. E* **54**, R2228 (1996); A. Neiman *et al.*, *Phys. Rev. Lett.* **76**, 4299 (1996); F. Chapeau-Blondeau, *Phys. Rev. E* **55**, 2016 (1997); J. Robinson *et al.*, *Phys. Rev. Lett.* **81**, 2850 (1998).
  - [4] J. Collins *et al.*, *Phys. Rev. E* **52**, R3321 (1995); *Nature (London)* **376**, 236 (1995); J. Levin and J. Miller, *Nature (London)* **380**, 165 (1996); D. Chialvo *et al.*, *Phys. Rev. E* **55**, 1798 (1997); L. Gammaitoni, *Phys. Rev. E* **52**, 4691 (1995).
  - [5] For reviews, see, e.g., L.A. Sagan, *Electric and Magnetic Fields: Invisible Risks?* (Gordon and Breach, Amsterdam, 1996); T. Akerstedt, B. Arnetz, G. Ficca, and P. Lars-Eric, *Sleep Res.* **26**, 260 (1997). Review report by the National Institute of Health is available at [http://www.niehs.nih.gov/emfrapid/html/WGReport/PDF\\_Page.html](http://www.niehs.nih.gov/emfrapid/html/WGReport/PDF_Page.html)
  - [6] S. Fauve and F. Heslot, *Phys. Lett.* **97A**, 5 (1983).
  - [7] B. McNamara and K. Wiesenfeld, *Phys. Rev. A* **39**, 4854 (1989).
  - [8] The noise was band limited at 10 kHz and ac coupled to the Schmitt trigger.
  - [9] The signal output power is defined as the spectral power at the fundamental frequency  $\omega_S$  (which was taken to be 64 Hz) minus the continuous noise background power within a small frequency range at about  $\omega_S$ ; it is a measure of the height of the signal feature above the noise background.
  - [10] The rate function  $f$  will depend on the specific system under investigation.
  - [11] J.W.S. Rayleigh, *The Theory of Sound* (Dover, NY, 1945), Vol. 2, Chap. 23.
  - [12] A. Grigorienco, P. Nikitin, and V. Roshchepkin, *Sov. Phys. JETP* **85**, 343 (1997).
  - [13] B.J. Gluckman *et al.*, *J. Neurophysiol.* **76**, 4202 (1996); *Phys. Rev. Lett.* **77**, 4098 (1996).